MATHEMATICAL MODELING OF THE CHEMICAL VAPOR INFILTRATION PROCESS

ANDREW D. JONES & PIERRE NGNEPIEBA, FLORIDA A&M UNIVERSITY, TALLAHASSEE, FL 32307
TALITHA M. WASHINGTON, UNIVERSITY OF EVANSVILLE, EVANSVILLE, IN 47722
DERRICK K. ROLLINS, SR., IOWA STATE UNIVERSITY, AMES, IA 50011

ABSTRACT

The Chemical Vapor Infiltration (CVI) process produces high performance ceramic composite materials. This process involves running a gas into a pyrolosis chamber at high temperatures to cause desired reactions within preforms of various shapes and chemical compositions. Achieving the desired pore filling in the least amount of time requires modeling and subsequent optimization of the reaction parameters such as temperature, pressure, and initial porosity of the preform. In this paper we present a model that describes gas transport phenomena, reaction kinetics and pore filling. With very few assumptions, the model predicts the concentration of gas molecules and the void in the preform. The proposed mathematical model yields a straight forward numerical algorithm that accurately simulates the process.

Keywords: Pyrolytic carbon; Chemical vapor deposition; Chemical vapor infiltration.

1. INTRODUCTION

The isothermal-isobaric carbon-carbon Chemical Vapor Infiltration (CVI) processes produce lightweight high performance ceramic composites. The materials have properties that include high thermal resistance, high mechanical strength, low coefficient of thermal expansion, low coefficient of friction and high chemical resistance. These composite materials are used for the nose cones of fighter jets, rocket thrusters, aircraft break pads, fuel cells and space shuttle tiles.

We examine a carbon-carbon CVI process that begins by raising the temperature of a graphite preform to a constant temperature in a reactor filled with argon gas. Propylene gas at room temperature but at equal pressure is connected to the reactor. The valve is then opened to allow the diffusion of the gas into the reactor and the preform. When the gas reaches equilibrium temperature with the system, the gas begins to disassociate and associate readily to form larger and smaller hydrocarbons. During this process, gas-solid reactions occur which leads to the densification of the preform.

A problem encountered is the inlet of the pore closing before the desired pore filling. This may be due to the large molecules reacting with the interior surface of the pore and sealing the inlet. Another cause is the reaction of hydrogen with the surface preventing the carbon molecules from bonding to the surface, or blocking of an active site. Lastly, the lightweight hydrogen products of heterogeneous and homogeneous reactions may diffuse back toward the inlet, pulling the hydrocarbon molecules closer to the inlet where they react with the surface to clog the pore.

Our model will be used to optimize the process using a variety of hydrocarbon precursors and industrial processes. The optimization code will produce the parameters that achieve the desired pore filling in the least amount of time. Since the molecules react with the surface of the pore, the model tracks the formation, transport and surface bonding of the molecules. We use this to calculate the void fraction as a function of space and time. In addition, the species of chemicals reacting with the substrate-hydrocarbon on graphite needed to be known and they react in temperatures around 1273-1373K and pressures around 50-60kPa. To minimize complexity of our model, we do not include the production of soot or bucky-balls, which are large nonreactive polyaromatic carbon rings that must be blown off the specimen after the reaction is complete in order to achieve greater densification.

For experimental and computational purposes, we assume that the preform is solid with uniform machined cylindrical pores. In addition, we assume that the gas transport is due to binary diffusion, pressure and concentration gradients. We use the Dusty-Gas Model to describe the mass transport and we assume that the

reduction of the void fraction occurs within each pore separately. Our model will be verified by experiments on prefabricated carbon performs.

2. Chemical Pathway

A reaction pathway has been proposed based on previous research on infiltration of carbon graphite with propylene (Li et al., 2005). The reaction rates are functions of temperature and pressure. Argon is used as a carrier gas at a temperature of 1273K and a pressure between 50-60kPa. Our model assumes that the reaction rates between the surface and aromatic molecules is much greater than the reaction rate between the surface and smaller hydrocarbons. The goal is to have large molecules form deep inside the pore thus filling the preform from the inside out.

This leads to a pathway describing the simplest formation of aromatic and poly-aromatic hydrocarbons from acetylene, propylene or other precursors. We include a reduced set of intermediate hydrocarbons to approximate the total gas composition.

3. Mathematical Model of Chemical Species

The mathematical model governing the change in the number molecules with respect to time is given by the following continuity equation.

$$\frac{\partial(\epsilon C_i)}{\partial t} = \vec{\nabla} \cdot \vec{N_i} + \sum_{i,j} k_i C_j - k_{is} C_i \tag{3.1}$$

The dimensionless void fraction ϵ is defined in terms V, the volume of the void as a function of space and time, and V_0, the volume of the pore at $t = 0$ and is given by $\epsilon = \epsilon(x,t) = \frac{V}{V_0}$. The concentration and flux of species i are functions of space and time and are C_i and N_i, respectively. The reaction rate for the creation or decomposition species i in the gas phase is denoted by k_i and k_{is} is the reaction rate of species i with the surface. The reaction rates k_i and k_s are Arrhenius functions of the temperature and have the following form.

$$k = k(x) = Ae^{-E/RT}$$

where A is the proportionality constant, E is the activation energy, R is the gas constant and T is the temperature. Note that $T = T(x)$ is a function of space for steady state thermal gradient CVI. For isothermal CVI, T is constant.

3.1. *Initial and Boundary Conditions.*

First we determine the initial concentrations and concentration gradients. Let C_1 denote the concentration of the precursor gas and assume that its normalized concentration does not change at the inlet.

$$C_1(0,t) = 1 \tag{3.1.1}$$

We assume that there is only one gas at the inlet and that there are no other gasses in the system initially. For $1 < i < n-1$, let C_i be the concentration of the gasses that result from chemical reactions. Let C_{n-1} denote the concentration of the hydrogen gas liberated by gas-gas and gas-solid reactions. Thus we have the following conditions.

$$C_2(0,t) = C_3(0,t) = \cdots = C_{n-1}(0,t) = 0 \tag{3.1.2}$$

$$C_2(x,0) = C_3(x,0) = \cdots = C_{n-1}(x,0) = 0 \tag{3.1.3}$$

Let C_n denote the concentration of the inert carrier gas and we assume that the preform and the entire reactor chamber is filled with this gas initially.

$$C_n(x,0) = 1 \tag{3.1.4}$$

From the given initial conditions we have the initial concentrations and we can solve for the concentration gradient at $t = 0$. Note that

$$\frac{\partial C_1(0,t)}{\partial x} \approx -\frac{C_1(0,t)}{\Delta x}, \tag{3.1.5}$$

$$\frac{\partial C_i(0,t)}{\partial x} = 0 \text{ for } 1 < i < n \tag{3.1.6}$$

and

$$\frac{\partial C_n(0,t)}{\partial x} \approx \frac{C_n(0,t)}{\Delta x} \tag{3.1.7}$$

where Δx is determined by the size of the spacial discretization.

The flux out at the right hand boundary is given by

$$\frac{\partial C_i(1,t)}{\partial x} = F D_{K_i} C(1,t)\epsilon(1,t) \tag{3.1.8}$$

where the constant of proportionality, F, is determined by comparing the numerical results with experimental data and solving the resulting inverse problem.

3.2. ***The Flux.***

Second, we calculate the flux term. We use the Dusty-Gas model to describe the flux due to binary diffusion and Knudsen diffusion as well as incorporates concentration and pressure gradients

$$-\frac{N_i}{D_{K_i}} = \frac{RT}{P}\sum_{j\neq i}\frac{C_i N_j - C_j N_i}{D_{ij}} + \frac{C_i B_e}{\mu D_{K_i}}\nabla P + \nabla C_i \tag{3.2.1}$$

where B_e is the permeability of the porous media, μ is the viscosity of the mixture, and P and T are the pressure and temperature for the system. The effective binary diffusivity for species i and j and the effective Knudsen diffusivity of species i are given by D_{ij} and $D_{K_i} = D_{K_i}(\epsilon)$, respectively.

The binary diffusion constant D_{ij} can be calculated by

$$\frac{P D_{ij}}{(P_{ci})^{\frac{1}{3}}(T_{ci}T_{cj})^{\frac{5}{12}}(\frac{1}{M_i}+\frac{1}{M_j})^{\frac{1}{2}}} = a\left(\frac{T}{\sqrt{T_{ci}T_{cj}}}\right)^b \tag{3.2.2}$$

where M is the molar mass, P_c is the critical pressure, T_{ci} and T_{cj} are the critical temperatures for the respective molecules i and j.

The Knudsen diffusivity constant D_K is a function of the pore radius, temperature and molecular weight. The Knudsen diffusion for the i^{th} species is given by

$$D_{K_i} = d(\epsilon)\sqrt{\frac{8RT}{9\pi M_i}\times 10^6} \tag{3.2.3}$$

where $d(\epsilon)$ is the diameter of the pore as a function of ϵ, the void fraction R is the universal gas constant, T is the temperature of the system, and M is the molar mass times a conversion factor of 10^6 for unit equivalence with the binary diffusion constant (Bird et al., 2002).

We simplify equation 3.2.1 by letting $F_P = \frac{B_e}{\mu}\nabla P$ and $v = \frac{RT}{P}$. (Note that if the flux due to a pressure gradient is zero then $F_p = 0$ and v is the molar volume of an ideal gas.) Thus, equation 3.2.1 becomes

$$N_i + vD_{K_i}\sum_{i\neq j}^{n}\frac{C_j N_i - C_i N_j}{D_{ij}} = -D_{K_i}\nabla C_i - F_P C_i \tag{3.2.4}$$

which leads to the following system of equations.

$$N_1 + vD_{K_1}\left(\frac{C_2N_1 - C_1N_2}{D_{12}} + \frac{C_3N_1 - C_1N_3}{D_{13}} + \cdots + \frac{C_nN_1 - C_1N_n}{D_{1n}}\right) = -D_{K_1}\nabla C_1 - F_P C_1$$

$$N_2 + vD_{K_2}\left(\frac{C_1N_2 - C_2N_1}{D_{21}} + \frac{C_3N_2 - C_2N_3}{D_{23}} + \cdots + \frac{C_nN_2 - C_2N_n}{D_{2n}}\right) = -D_{K_2}\nabla C_2 - F_P C_2$$

$$\vdots$$

After rearrangement of terms we have

$$\left[1+vD_{K_1}\left(\frac{C_2}{D_{12}}+\frac{C_3}{D_{13}}+\cdots\frac{C_n}{D_{1n}}\right)\right]N_1-\frac{vD_{K_1}C_1}{D_{12}}N_2-\frac{vD_{K_1}C_1}{D_{13}}N_3-\cdots-\frac{vD_{K_1}C_1}{D_{1n}}N_n=-D_{K_1}\nabla C_1-F_PC_1$$

$$-\frac{vD_{K_2}C_2}{D_{21}}N_1+\left[1+vD_{K_2}\left(\frac{C_1}{D_{21}}+\frac{C_3}{D_{23}}+\cdots\frac{C_n}{D_{2n}}\right)\right]N_2-\frac{vD_{K_2}C_2}{D_{23}}N_3-\cdots-\frac{vD_{K_2}C_2}{D_{2n}}N_n=-D_{K_2}\nabla C_2-F_PC_2$$

$$\vdots$$

which simplifies to

$$\left(1+vD_{K_i}\sum_{j=1,j\neq i}^{n}\frac{C_j}{D_{ij}}\right)N_i-vD_{K_i}C_i\sum_{j=1,j\neq i}^{n}\frac{N_j}{D_{ij}}=-D_{K_i}\nabla C_i-F_PC_i \tag{3.2.5}$$

for $i=1,...,n$.

For the off diagonal elements let

$$a_{ij}=-\frac{vD_{K_i}C_i}{D_{ij}},\quad \text{if } i\neq j$$

and for the diagonal elements let

$$a_{ii}=1-\sum_{j=1,j\neq i}^{n}a_{ij}=1+vD_{K_i}\sum_{j=1,j\neq i}^{n}\frac{C_j}{D_{ij}},\quad \text{if } i=j$$

and define the matrix $A=[a_{ij}]$.

Recall that the flow is axial symmetric so that

$$\nabla C=\frac{\partial C}{\partial x}\text{ and }\nabla P=\frac{\partial P}{\partial x}.$$

Now let

$$b_i=-D_{K_i}\nabla C_i-F_pC_i=-D_{K_i}\frac{\partial C_i}{\partial x}-\frac{B_e}{\mu}\frac{\partial P}{\partial x}C_i$$

and define the vector $B=[b_i]$. Thus, we have the system

$$a_{11}N_1+a_{12}N_2+a_{13}N_3+\cdots+a_{1n}N_n=b_1$$

$$a_{21}N_1+a_{22}N_2+a_{23}N_3+\cdots+a_{2n}N_n=b_2$$

$$a_{31}N_1+a_{32}N_2+a_{33}N_3+\cdots+a_{3n}N_n=b_3$$

$$\vdots\qquad\vdots\qquad\vdots\qquad\qquad\vdots\qquad\vdots$$

$$a_{n1}N_1+a_{n2}N_2+a_{n3}N_3+\cdots+a_{nn}N_n=b_n$$

or

$$\begin{bmatrix}a_{11}&a_{12}&a_{13}&\cdots&a_{1n}\\a_{21}&a_{22}&a_{23}&\cdots&a_{1n}\\a_{31}&a_{32}&a_{33}&\cdots&a_{1n}\\\vdots&\vdots&\vdots&\ddots&a_{1n}\\a_{n1}&a_{n2}&a_{n3}&\cdots&a_{nn}\end{bmatrix}\begin{bmatrix}N_1\\N_2\\N_3\\\vdots\\N_n\end{bmatrix}=\begin{bmatrix}b_1\\b_2\\b_3\\\vdots\\b_n\end{bmatrix}$$

Thus,

$$AN = B \tag{3.2.6}$$

where the flux vector is $N = [N_i]$. The flux of each species is then determined by $N = A^{-1}B$.

3.3. *Change in Gases.*

Now that we have the flux for each species, we can calculate the change in the number of molecules with respect to time due to the flux and chemical reactions. We do this for a reduced reaction set where $n = 7$. Let $C_1 = C_3H_6$, $C_2 = CH_4$, $C_3 = C_2H_4$, $C_4 = C_2H_2$, $C_5 = C_6H_6$, $C_6 = H_2$, and $C_7 = Ar$. Since solid graphite is much denser than the hydrocarbon gas we assume that $\frac{\partial(\epsilon C_i)}{\partial t} << \epsilon\frac{\partial C_i}{\partial t}$ and treat the temporal change in the void fraction separately. Again, since a cylinder is axial symmetric, we consider flow in one dimension. Finally, consider the following reduced reaction network:

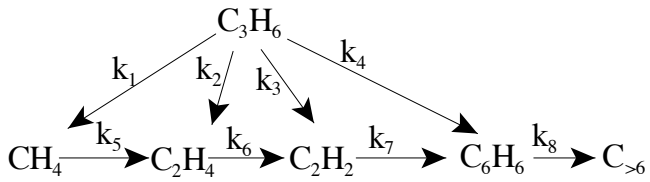

Figure 1. A parallel/series-consecutive reaction model for propylene pyrolysis.

Thus, the continuity equation for each species is:

$$\epsilon\frac{\partial C_1}{\partial t} = \frac{\partial N_1}{\partial x} - [k_1 + k_2 + k_3 + k_4]C_1 - k_{1s}C_1 \tag{3.3.1}$$

$$\epsilon\frac{\partial C_2}{\partial t} = \frac{\partial N_2}{\partial x} + k_1C_1 - k_5C_2 - k_{2s}C_2 \tag{3.3.2}$$

$$\epsilon\frac{\partial C_3}{\partial t} = \frac{\partial N_3}{\partial x} + k_2C_1 + k_5C_2 - k_6C_3 - k_{3s}C_3 \tag{3.3.3}$$

$$\epsilon\frac{\partial C_4}{\partial t} = \frac{\partial N_4}{\partial x} + k_3C_1 + k_6C_3 - k_7C_4 - k_{4s}C_4 \tag{3.3.4}$$

$$\epsilon\frac{\partial C_5}{\partial t} = \frac{\partial N_5}{\partial x} + k_4C_1 + k_7C_4 - k_8C_5 - k_{5s}C_5 \tag{3.3.5}$$

$$\begin{aligned}\epsilon\frac{\partial C_6}{\partial t} = \frac{\partial N_6}{\partial x} &+(-3k_1 + \frac{3}{2}k_3 + \frac{3}{2}k_4)C_1 + k_5C_2 + k_6C_3 + \\ &+3k_{1s}C_1 + 2k_{2s}C_2 + 2k_{3s}C_3 + k_{4s}C_4 + 3k_{5s}C_5\end{aligned} \tag{3.3.6}$$

The flux due to binary diffusion and concentration gradients of the inert gas Argon are the only contribution to its change in concentration and its equation is given by the following.

$$\epsilon\frac{\partial C_7}{\partial t} = \frac{\partial N_7}{\partial x} \tag{3.3.7}$$

3.4. *Change in the Solid.*

To model the temporal evolution of the solid we let

$$-\frac{\partial \epsilon}{\partial t} = p_1C_1k_{1s}V_{M_1} + p_2C_2k_{2s}V_{M_2} + p_3C_3k_{3s}V_{M_3} + p_4C_4k_{4s}V_{M_4} + p_5C_5k_{5s}V_{M_5} \tag{3.4.1}$$

where V_{M_i} is the molecular volume of species i. p_i is a proportionality constant that is equal to the probability of a collision of the gas with the solid for a given concentration, temperature and surface to volume ratio.

3.5. ***The Numerical Algorithm.***

Given the initial concentrations, $C_i(x,0)$ and initial concentration gradients $\frac{\partial C_i(x,0)}{\partial x}$ we can calculate the flux at the first time step $N_i(x,t_1)$. Now that we have the flux $N_i(x,t_1)$, we compute the consumption and creation of molecules form the gas-gas and gas-solid reactions and hence $\dfrac{\partial\left[\epsilon C_i(x,t_1)\right]}{\partial t}$. We assume that the gas is stationary for a small time Δt and compute the change in the void from the gas-solid reaction. From this we compute $\varepsilon\left(x,t_1\right)$. With $\varepsilon\left(x,t_1\right)$ we update the Knudsen diffusivity $D_{K_i}(\epsilon)$ and repeat the process until $\varepsilon\left(x,t\right)\approx 0$ for some $x\in[0,1]$.

4. Experimental Design for Verification of Model

We constructed a model with practical experimental conditions in mind. We will run experiments that correspond the mathematical model. To satisfy the left had boundary condition $C_1(0,t)=1$ we adjust the pressure so that the flux due to the pressure gradient it is slightly greater than the flux due to binary diffusion and the flux due to concentration gradients.

$$\frac{C_i B_e}{\mu D_{K_i}}\nabla P > \frac{RT}{P}\sum_{j\neq i}\frac{C_i N_j - C_j N_i}{D_{ij}} + \nabla C_i$$

This pressure gradient keeps the gas flowing in one direction. With this adjustment the impact of hydrogen blocking active sights is greatly reduced. We assume that the pressure is a linear function of space and is independent of the pore diameter. Thus, the pressure gradient is constant in space and time. We end the experiment when the pore diameter is small at any point in the pore. The temperature will be kept constant.

First, we will construct and run experiments to verify the concentration of the gas species as a function of space and time with no preform in the reactor. Second, we will experimentally determine the gas-solid reaction rates. Finally, we infiltrate the cylindrical pores.

5. Conclusion

The assumption that the change is the concentration of gas with respect to time is much greater than the change in the void with respect to time is valid for all practical experiments. For isobaric CVI the boundary condition at the inlet $C_1(0,t)=1$ will need to be modified. For CVI where the right hand boundary, $x=1$ is closed, e.g. deep coatings, the proportionality constant F will be zero and hydrogen-solid reaction will be taken into account.

We have proposed a mathematical model of the Chemical Vapor Infiltration process with few simplifying assumptions that yields a straight forward numerical algorithm that is experimentally verifiable. The model allows for both a thermal and a pressure gradient and takes into account the flux. The model is then compared to experimental data and refined, and will be extended to the case where the void at $x=1$ is zero. That is, where hydrogen blocks active sites. We will then consider a reduced reaction network that includes 44 species of hydrocarbon and solve the resulting system with $n=46$ (cf sec. 3.3). Optimal control will be applied to the resulting model to produce the desired composite product in the minimal amount of time.

Acknowledgments

This research was funded under contract of the Future Affordable Multi-Utility Vehicle program at Florida Agriculture and Mechanical University (FAMU). This funding was included in the Department of Defense Appropriations Act.

References

Becker, A. and K.J. Huttinger. 1998. Chemistry and Kinetics of Chemical Vapor Deposition of Pyrocrbon-III Pyrocarbon Deposition from Propylene and Benzene in the Low Temperature Regime. Carbon 36:177-199.

Becker, A. and K.J. Huttinger. 1998. Chemistry and Kinetics of Chemical Vapor Deposition of Pyrocrbon-II Pyrocarbon Deposition from Ethylene, acetylene and 1,3-Butadiene in the Low Temperature Regime Carbon. Carbon 36:201-211.

Birakayala N. and E. A. Evans. 2002. A Reduced Reaction Model for Carbon CVI/CVD Processes. Carbon 40:675-683.

Bird R, W. Stewart, and E. Lightfoot. 2002. Transport Phenomena, 2nd Ed., John Wiley & Sons, Inc.

Jackson R. 1977. Transport in Porous Catalysts. Elsevier Science Publisher.

Jones, A.D. 2007. Estimates for the Void Fraction during the Chemical Vapor Infiltration Process. WSEAS Transactions on Mathematics Volume 6, Issue 4, April 2007

Jones, A.D. In Press. Profile of an Unsuccessful Process and the Criteria for a Successful Process for the Chemical Vapor Infiltration Process. Applied Mathematical Modeling.

Li, H., A. Li, R. Bai, and K. Li. 2005. Numerical Simulation of Chemical Vapor Infiltration of Propylene into C/C Composites with Reduced Multi-Step Kinetic Models. Carbon 43:2937-2950.

National Institute of Standards and Technology Chemical Kinetics Database on the Web Standard Reference Database 17, Version 7.0 (Web Version), Release 1.2.